Journal of Alloys and Compounds 509 (2011) 8501–8509

Contents lists available at ScienceDirect

Journal of Alloys and Compounds

journal homepage: www.elsevier.com/locate/jallcom

Electronic characterization and reactivity of bimetallic clusters of the Ti(Mg)$_n$ type for hydrogen storage applications

Wilber Silva [a], Thanh N. Truong [b], Fanor Mondragon [a,*]

[a] Institute of Chemistry, University of Antioquia, A.A. 1226, Medellin, Colombia
[b] Henry Eyring, Center for Theoretical Chemistry, Department of Chemistry, University of Utah, 315 South 1400 East, Rm 2020, Salt Lake City, UT 84112, USA

ARTICLE INFO

Article history:
Received 11 March 2011
Received in revised form 2 May 2011
Accepted 6 June 2011
Available online 15 June 2011

Keywords:
Magnesium cluster
Bimetallic titanium–magnesium
Hydrogen storage

ABSTRACT

This paper describes the variations in the properties, characteristics and hydrogenation energy barriers of magnesium clusters induced by titanium. DFT approach was used to determine the most stable structures at this theory level and then MP2 was used to refine the energy calculations with the basis set 6-311g(d) for magnesium and hydrogen, and pseudopotential lanl2dz for titanium. Bimetallic clusters showed higher stability and reactivity than the corresponding magnesium ones. Titanium induces a change in the magnesium atoms in their electronic configuration reflected in an increase of the population of their orbitals. At the same time titanium electronic populations is modified. These changes cause variations in some reactivity parameters such as the Fukui indexes which modify the hydrogenation of the magnesium clusters and bimetallic clusters. For example, there is a reduction in the energy barrier for dissociation of the H_2 molecule in the bimetallic clusters. In the hydrogenated cluster the hydrogen atoms form bridges between all of the magnesium or magnesium–titanium atoms. These results indicate that, energetically, bimetallic systems can be more promising systems for hydrogen storage.

1. Introduction

The development of hydrogen as an energy vector requires systems with hydrogen storage capability of more than 7% in weight (w/w) at near ambient conditions [1]. Different approaches have been proposed such as high-pressure tanks [1,2], high surface area materials [3–8] and materials for chemical absorption [9–14] such as metal hydrides. Among many potential hydrogen storage materials, those based on magnesium [15] are of particular interest because magnesium has a high hydrogen storage capacity and also has one of the lowest decomposition temperatures among the hydride compounds. However, the low decomposition-formation kinetics of the magnesium hydride and slow diffusion of hydrogen through the magnesium crystal tend to limit its practical application [16].

Experimental data obtained with pure magnesium nanoparticles of about 2.5 nm show a reduction in the hydrogenation temperature from 380 °C to values around 250 °C [17]. Other studies show that dehydrogenation reactivity of MgH_2 is directly dependant on the particle size [18]. The hydrogenation of pure magnesium has been investigated using computational chemistry calculations, some of these results indicate that reactivity of particles with a diameter less than 1.0 nm (about 15 Mg atoms), estimated by molecular dynamic studies, is very different from the one observed for bigger size particles [19]. DFT calculations carried out by Wagemans et al. [20] showed that for nano-sized clusters with about 15 magnesium atoms, the hydrogenation energy can be as low as 18 kcal/mol. The higher reactivity and small hydrogenation energy are factors that favor the reduction in the hydrogenation temperature of small Mg clusters.

On the other hand, since the work of Reilly and Wiswall [21,22] on the hydrogenation of different magnesium alloys, with transition metals, there has been a growing interest to find better combinations of magnesium with doping metals to improve the hydrogenation–dehydrogenation kinetics and to decrease its decomposition temperature. In this way, different materials have been developed such as alloys or mixtures with other materials trying to obtain similar or better hydrogen storage capacities, under more mild conditions, and at the same time to obtain higher adsorption–desorption kinetics than those obtained with pure magnesium hydride. Thermogravimetric studies show that Fe–Mg alloys have faster hydrogenation reaction kinetics than that of pure magnesium [23,24]. In the case of vanadium–magnesium alloys the reduction in the hydrogenation temperature can be close to 100 °C [25], particularly in systems with particle size in the range of nanometers. Similar tendency has been observed in the case of magnesium alloys with Ni [26,27] and Ti [28,29] as well as with other compounds [30,31]. Computational calculations in

* Corresponding author. Tel.: +57 4 219 6614; fax: +57 4 219 6565.
E-mail address: fmondra@udea.edu.co (F. Mondragon).

0925-8388/$ – see front matter © 2011 Elsevier B.V. All rights reserved.
doi:10.1016/j.jallcom.2011.06.022

which a magnesium atom of the cluster was replaced by an atom of a transition metal were used to investigate the electronic and thermodynamic properties of the hydrogenation of these alloys by Chen et al. [32]. Most of the transition metals were found to stabilize the hydrogenated Mg crystal array with the exception of Sc, Y and Zr. Among the investigated metals Ti, V, Fe and Ni were found to improve reactivity and stability of the doped magnesium crystals for hydrogenation, in some cases similar to the reactivity of the pure metals.

However, questions on whether the effects of metal on the activity of the magnesium cluster as a function of the cluster size and on the overall physical and chemical properties of the alloy nanoparticles have not been addressed fully. To get further understanding of these properties, in this study we examined electronic, thermodynamic and hydrogenation characteristics of $Ti(Mg)_n$ clusters with less than 7 magnesium atoms using electronic structure methods.

2. Computational approach

2.1. Characterization of the magnesium and titanium–magnesium clusters

The initial geometries of the clusters before optimization were based on the symmetry and geometry data of Mg and bimetallic clusters published in the literature [33–35], then a set of different structures with different geometries and different full point symmetry group were generated for each cluster size. The structures of each cluster size were fully optimized using the hybrid density functional theory (DFT) with the functional B3PW91 and the pseudopotential Lanl2dz basic set, all calculations were performed using the software Gaussian 03 [36]. This DFT method has been suggested in the literature as one of the most appropriate for the analysis of Mg clusters [37] and it is one of the best options to search geometries in systems with transition metals [38], while the pseudopotential is suitable for the description of relativistic effects in metals with part full *d* orbitals [39]. Each cluster was characterized in different electronic states—quintuplet, triplet and singlet. This information was used to find the minima of each type of cluster. Although, under normal conditions, clusters of different electronic states can contribute to the overall chemistry of the system, for simplicity in this study, we considered only contributions of electronic states of the lowest energy state (ground-state) of the clusters. The clusters selected in this way were used for the hydrogenation reactions. The hydrogenation process was carried out by adding two hydrogen atoms at the same time. With this procedure, we explored a set of different geometrical configurations based in cluster symmetry in order to decide where the two hydrogen atoms were adsorbed. This procedure generates a large number of different structures which were optimized with the same DFT method and the structure with the lowest energy were selected, then, another two hydrogen atoms were added and the optimization process repeated until the whole cluster was saturated (Mg_nH_{2n}). Only the lowest energy structures were reported. Energy data were further improved by single-point energy calculations at MP2 level of theory using the basic set 6-311g(d) for the Mg atoms and Lanl2dz for the Ti atom.

Molecular hydrogen dissociation was studied to determine the possible effect of Ti in the kinetics of the process. For each stable cluster, we explored a set of possible ways by which the hydrogen molecule can be dissociated. This was done using scan calculations to determine possible transition states. In this procedure the hydrogen molecule approached the cluster in a face, bond, atom, or another possible configuration. After identifying and characterizing the transition state, we did an IRC calculation with the same level of theory to verify the reaction path.

2.2. Theoretical models for reactivity

Density functional theory allows the calculation of some chemical reactivity indices such as chemical potential (μ), chemical hardness (η) and the Fukui function. The chemical potential and chemical hardness relate the first and second derivative of energy with respect to the number of electrons at the potential constant ($v(r)$) – by the following: [40].

$$\mu = \left(\frac{\partial E}{\partial N}\right)_{v(r)} \tag{1}$$

$$\eta = \frac{1}{2}\left(\frac{\partial^2 E}{\partial N^2}\right)_{v(r)} = \frac{1}{2}\left(\frac{\partial \mu}{\partial N}\right)_{v(r)} \tag{2}$$

It is also possible to obtain both parameters using the Koopmans approximation with the frontier orbitals of a chemical species as follows:

$$\mu = \frac{1}{2}(\mathrm{IP} + \mathrm{EA}) \approx \frac{1}{2}(\varepsilon_\mathrm{L} + \varepsilon_\mathrm{H}) \tag{3}$$

$$\eta \approx \frac{1}{2}(\mathrm{IP} - \mathrm{EA}) \approx \frac{1}{2}(\varepsilon_\mathrm{L} - \varepsilon_\mathrm{H}) \tag{4}$$

where IP is the ionization potential, EA is the electron affinity while ε_H and ε_L are the HOMO and LUMO orbital energies, respectively. Both properties describe the tendency of a chemical species to receive/transfer its electron from/to another. The chemical potential shows the direction in which the electron transfer can take place, while the chemical harness indicates the ability of accepting electron. A hard molecule does not easily accept electrons.

Fukui function is a local reactivity index that can also be evaluated using DFT. This reactivity index is determined by the electronic characteristics of the frontier HOMO or LUMO electron density by the following expression [40,41].

$$f = \left(\frac{\delta \mu}{\partial v(r)}\right)_N = \left(\frac{\partial \rho(r)}{\partial N}\right)_{v(r)} \tag{5}$$

$$f^-(r) \approx \rho_{(\mathrm{HOMO})}(r) \tag{6}$$

A large value of f at a given site favors reactivity at that point. In this research the Fukui function was calculated using the Top-Mod software [42] taking into account the wave function of the lowest energy configurations.

3. Results and discussion

3.1. Geometrical and electronic properties of magnesium and titanium–magnesium clusters

The most stable structures of the bimetallic clusters, investigated in this research with just one Ti atom, were in quintuplet state. Singlet and triplet electronic states were also evaluated; however, their energy values were higher than the quintuplet state. There are some stable structures in triplet state which differ just a few kcal/mol from that of the quintuplet state. There are some stable structures in triplet state which differ just a few kcal/mol from that of the quintuplet state, see Supplementary information.

Fig. 1 shows magnesium clusters where one of the Mg atoms was substituted by one Ti atom. Each one of these clusters can have different isomers. However, those presented here are the energetically most stable ones in relation to each cluster size.

The most stable structures with more than four atoms are tridimensional, no stable planar structures were found for clusters with more than 4 atoms. In none of the optimized clusters does the Ti atom appear as the central atom; it is always located at the surface of the cluster. In the optimization, no linear clusters were found

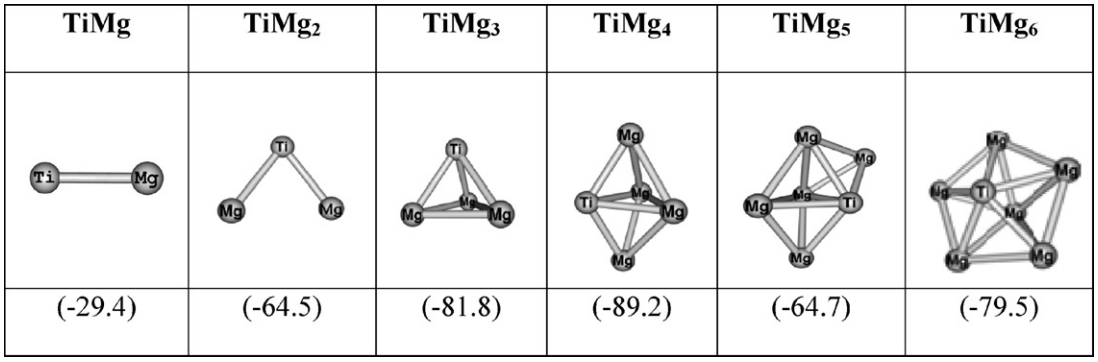

Fig. 1. Most stable isomers of $TiMg_n$ clusters. In parenthesis, the energy, in kcal/mol, of the addition of a Ti atom to the Mg cluster: $Ti + Mg_{(n+1)} \rightarrow TiMg_n + Mg$.

Table 1
Variation of the electronic configuration and charge of the titanium atom in the titanium–magnesium clusters.

Number of Mg atoms	Ti electronic configuration $4s^2 3d^2 4p^0 4d^0$	NBO charge
1	$4s^{0.30}3d^{3.01}4p^{0.62}4d^{0.05}$	0.032
2	$4s^{0.85}3d^{2.51}4p^{0.86}4d^{0.06}$	−0.270
3	$4s^{0.59}3d^{3.07}4p^{0.56}4d^{0.02}$	−0.228
4	$4s^{1.01}3d^{2.33}4p^{0.79}4d^{0.09}$	−0.216
5	$4s^{0.88}3d^{2.49}4p^{0.98}4d^{0.13}$	−0.464
6	$4s^{0.70}3d^{3.29}4p^{1.14}4d^{0.12}$	−1.242

suggesting that the atomic interactions can be very mild with low covalent character and more van der Waals type interaction [43]; the electronic configuration of Mg atoms in the clusters is presented in Table 1 of the Supplementary material. This information shows that the magnesium atoms in clusters smaller than 4 are closer to the $3s^2$ configuration of the atomic Mg. Therefore, van der Waals interactions are favored. The most stable clusters have C_s symmetry. There is loss of symmetry induced by the presence of the Ti atom which introduces different bond lengths.

Variation of the bond lengths of Ti–Mg and Mg–Mg of the most stable isomers is presented in Fig. 2. The Ti–Mg bond length remains almost constant with the size of the clusters here investigated. However, the Mg–Mg average bond length in the bimetallic cluster as well as in the pure Mg clusters decreases with the size of the cluster, approaching the value of 3.21 Å of the bulk Mg [37]. This reduction of the bond length with the size of the clusters indicates more stability of the larger clusters.

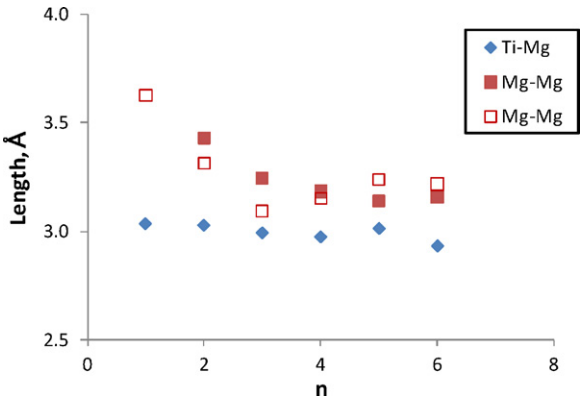

Fig. 2. Variation of the average bond length of Ti–Mg and Mg–Mg versus the size of the cluster. Filled symbols are for the bimetallic system. Open circles for the pure Mg clusters.

3.2. Electronic characterization

3.2.1. Global characteristics

3.2.1.1. Cohesion energy. The value of the average binding energy provides an idea of the stability of a cluster, this value is determined as the negative of the difference between the energy of the cluster and the energy of the elements (see Eq. (7)), the data thus obtained is presented in Fig. 3a).

$$\Delta E = -\frac{(E_{TiMgn} - E_{Ti} - nE_{Mg})}{(n+1)} \quad (7)$$

The presence of Ti in the cluster induces an energetic stability of about 15 kcal/mol per Mg atom compared to that of the pure magnesium cluster. This is an important effect that shows how this atom can distort the electronic structure of the magnesium atoms which induces a larger orbital overlapping between the Mg atoms.

3.2.1.2. Chemical hardness. The hardness of a chemical species (molecule, ion or atom) gives a qualitative description of how polarizable the species is when exposed to an electrical field. The concept has been particularly useful to understand the acid–base chemistry and also to interpret chemical reactivity.

Fig. 3b shows the variation of the chemical hardness of the $MgMg_n$ and $TiMg_n$ clusters with the size of the cluster. In general there is a tendency of the hardness to become smaller with the size of the cluster. The main differences are found in the smaller clusters, $n = 1$ or 2. The Ti atom in the cluster reduces the hardness of the small clusters and brings this parameter to values that show only a slight variation with the number of Mg atoms. This tendency suggests that in this kind of bimetallic clusters there is a small reduction of the energy required to transfer electronic charge to other systems as the size of the cluster increases.

3.3. Local characteristics

3.3.1. Variations of the Ti electronic configuration in the titanium–magnesium clusters

Table 1 shows the changes in the electronic configuration and the charge of the Ti atom in the titanium–magnesium clusters. The configuration of magnesium atoms is presented in the Supplementary material. There is a strong interaction between both metals which modifies the electronic properties of both atoms. The electronic configuration of the Ti atom shows that the presence of just one Mg atom causes a reduction in the charge of the 4s orbital from two to one or less electrons. At the same time the charge of the 3d orbital is augmented between 0.5 and 1.3 electrons depending on the type of cluster. The charge of the 4p orbital is also markedly increased particularly in the clusters with 5 and 6 Mg atoms. The charge of the 4d orbital is slightly modified. In general, the Ti atom

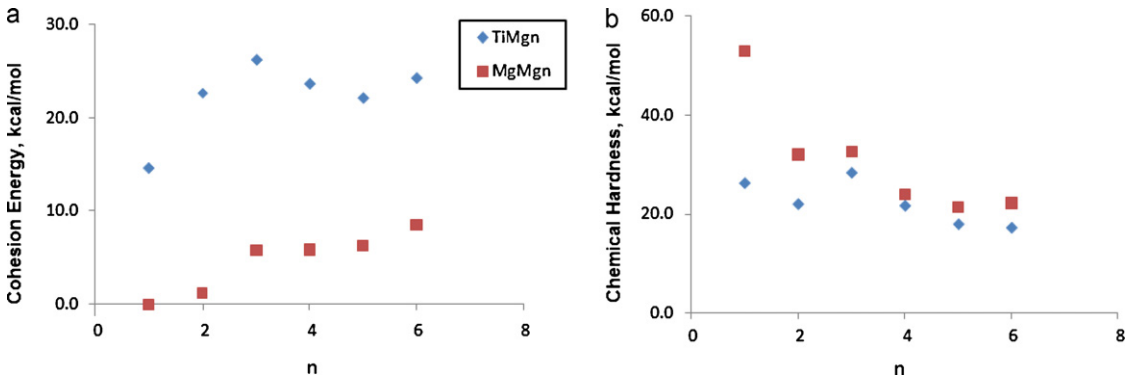

Fig. 3. (a) Average cohesion energy. (b) Chemical hardness.

gains charge from the Mg atoms and the value increases with the number of Mg atoms.

The analysis of the electronic configuration of the Mg atoms shows that the population of the s-orbital is drastically reduced to values between 1.5 and 1.0 electrons while the p-orbital has between 0.3 and 0.8 electrons. This is a large change in the electronic configuration considering that the energy required for the transfer of one electron from the 3 s orbital to the 3p orbital is more than 100.4 kcal/mol [44]. The changes in the electronic configuration of TiMg, $TiMg_2$ and $TiMg_3$ suggest that these variations are apparently controlled by the geometry of the cluster.

3.3.1.1. Cluster reactivity based on the Fukui function. Indexes such as hardness give an idea of global reactivity but these values do not indicate from which side the cluster grows or which atom or region of the cluster is the most susceptible to the attack of an electrophilic of nucleophilic species. This information can be obtained from the analysis of the Fukui function or frontier function.

The representation of the Fukui function is shown in Fig. 4. This kind of illustration displays the region of the cluster where the largest concentration of the electron density is located, and therefore is the area of highest reactivity in the cluster. If the reactivity is located in the frontier orbitals, the HOMO allows determining the value of the function f^- where an electrophilic attack may be oriented. In Fig. 4 the values of the Fukui function for the 0.02 isosurface are presented for the pure magnesium clusters ($Mg–Mg_n$) and the titanium magnesium clusters ($Ti–Mg_n$). The value and the shape of the Fukui function indicate the differences between both clusters. For this isosurface the smaller clusters are the most reactive. In both cases the common point is that the reactivity is not located on any specific atom, it is mostly directed towards the bonding between atoms or in the planes of the clusters. See for example the Mg_4 cluster where the reactivity is located between two of the bondings while in the $TiMg_2$ the reactivity is directed to both sides of the plane formed by the three atoms. In the other clusters, the reactivity appears more evenly distributed around the cluster. As expected, in the magnesium clusters the reactivity is more symmetrically distributed than in the clusters with Ti. One exception is the $TiMg_2$ cluster that has the same value of the f^- function on both sides of the cluster and no distortion is induced by the Ti atom as is the case for the other clusters where the f^- function is located towards the Ti atom. As mentioned before, the Fukui index indicates the most probable region of the cluster where a reaction can take place. When an atom is added to a cluster, the addition follows the direction indicated by the f^- function. However, due to the relaxation processes of the cluster during its optimization, there are changes in the geometry. For example, see in Fig. 4 the variations when going from $TiMg_2$ to $TiMg_3$ and to $TiMg_4$. This sequence suggests that the place where the new atom can be identified.

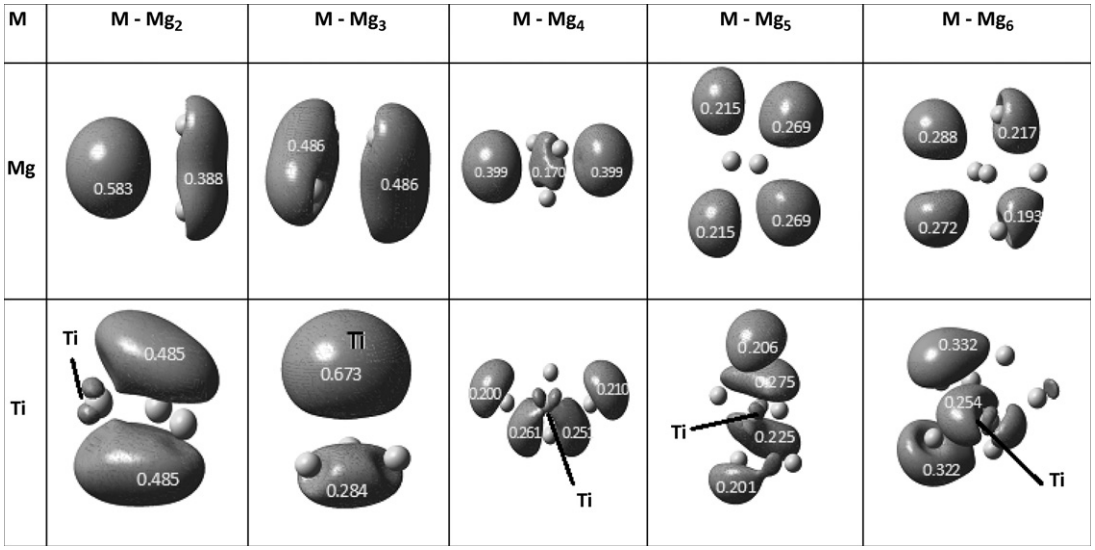

Fig. 4. Variations in the electronic density induced by the Ti atom. Isosurface representation of the Fukui function of the $Mg–Mg_n$ and $Ti–Mg_n$ clusters. Large f^- values indicate higher electronic density in that area of the cluster, and therefore, is the place of higher reactivity. The largest concentration of the electronic density is not necessarily associated with the Ti atom.

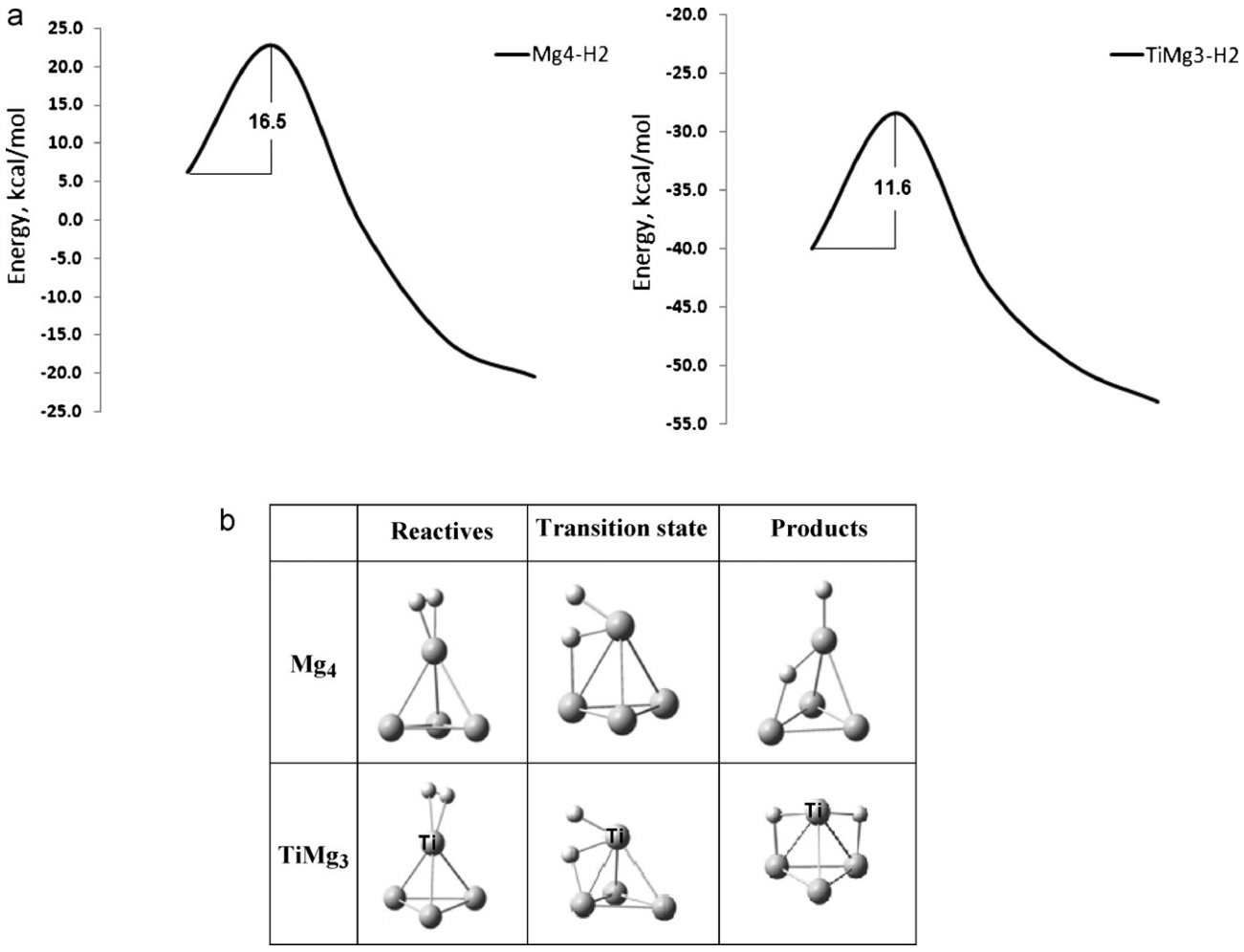

Fig. 5. (a) Potential energy surface for the dissociation of molecular hydrogen on the Mg–Mg_3 and Ti–Mg_3 clusters. (b) Structures illustrating the hydrogen chemisorptions, transition state and dissociation of the hydrogen molecule and hydrogen atom migration.

However, due to internal migrations in the cluster, the final geometry of the same cannot be assessed.

3.3.2. Effect of the Ti atom on the hydrogenation energy

To determine the hydrogenation properties of the magnesium and titanium–magnesium clusters, a relaxed scan was done as explained previously. In general there are two main steps, the first is the formation of a complex H_2–XMg_n which is followed by dissociation of the hydrogen molecule, and the second, the migration of the hydrogen atoms to other positions in the cluster. This migration takes place according to the previously described reactivity indexes.

Fig. 5a shows the potential energy surface for a hydrogen molecule dissociation in the clusters with four atoms (XMg_3). The analysis is done with this type of cluster because of the geometrical and structural similarities between the clusters with and without Ti which facilitates the comparison between them. However, the results can be extrapolated to other clusters. Dissociation of the first hydrogen molecule in the magnesium cluster has an energy barrier of about 17 kcal/mol. The transition state complex has an imaginary frequency of $-1576\,cm^{-1}$ indicating the direction of the H–H dissociation. The presence of the Ti atom reduces the energy barrier to about 12 kcal/mol, in this case the transition state complex has an imaginary frequency of $-579\,cm^{-1}$. In both cases the process is exothermic. The above results suggest that hydrogenation of the titanium–magnesium clusters can be kinetically more favorable than the hydrogenation of pure Mg clusters.

Hydrogen adsorption and dissociation is illustrated in Fig. 5b. The initial stage of the reaction of both clusters up to their transition state is rather similar. In both cases the transition state has one hydrogen atom bonded to two atoms, which coincide with the location of the highest value of the Fukui function. The other hydrogen atom is in a dangling position, as shown in Fig. 5b. The final product is slightly different due to a Ti induced re-orientation of the dangling atom to form two bonds. BSSE calculations were carried out finding a correction of 0.26 kcal/mol. Therefore the BSSE corrections were not included in the calculations.

3.3.3. Hydrogenation characteristics of the $TiMg_n$ clusters

Each cluster was hydrogenated until it became completely saturated. The smaller clusters have a larger capacity to adsorb hydrogen atoms. For example, the TiMg cluster can adsorb six hydrogen atoms to generate a stable structure with no imaginary frequencies (H/Mg ratio 6:1). The $TiMg_2$ can adsorb a maximum of eight hydrogen atoms (H/Mg ratio 4:1). This hydrogen adsorption capacity is reduced as the number of magnesium atoms is increased, the $TiMg_6$ cluster can take 12 hydrogen atoms for an H/Mg ratio of 2:1. The small size Ti–Mg clusters have the capacity to adsorb one extra hydrogen molecule compared to the equivalent pure magnesium cluster, see for example the $TiMgH_6$ and $TiMg_2H_8$ clusters, in both cases there is one hydrogen molecule adsorbed directly on the Ti atom. The difference is that in the $TiMgH_6$ the extra hydrogen molecule has the H–H bond completely dissociated while in the Ti Mg_2H_8 the H–H bond distance is similar to

a

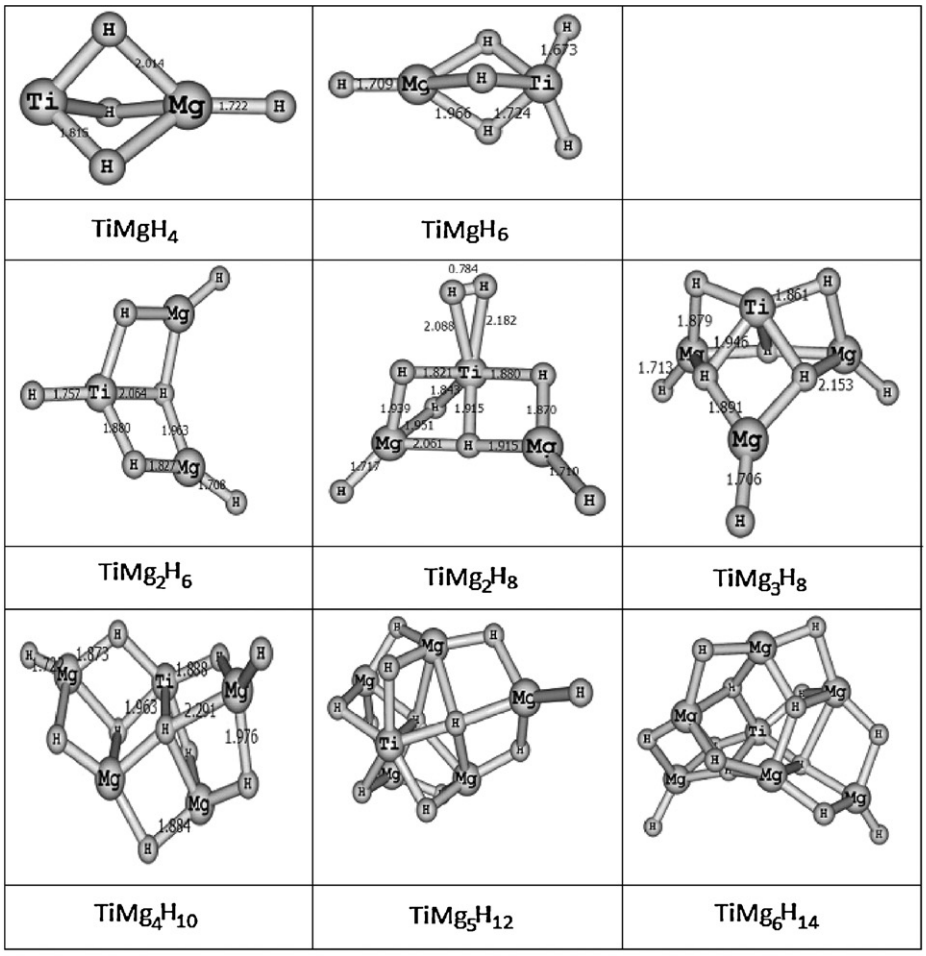

b

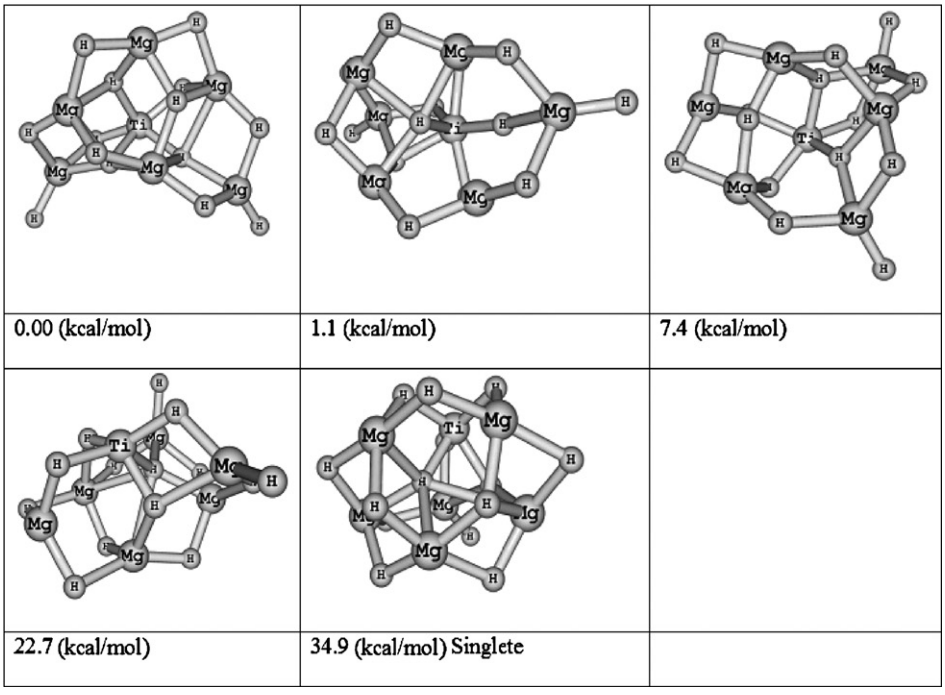

Fig. 6. Most stable hydrogenated isomers of $TiMg_n$. (a) Structures with the highest hydrogen uptake capacity. Observe the lack of symmetry in most of these structures. (b) Isomers of $TiMg_6H_{14}$.

Table 2
Ti–Mg average bond order determined using the Wiberg indexes.

Estructure		$TiMg$	$TiMg_2$	$TiMg_3$	$TiMg_4$	$TiMg_5$	$TiMg_6$
Wiberg index	Metallic cluster	0.605	0.715	0.610	0.523	0.545	0.552
	Hydrogenated clusters	0.139	0.080	0.070	0.093	0.119	0.062

that in molecular hydrogen. It is interesting to observe that in the hydrogenated clusters there is no direct bonding between the Ti atom and the Mg atoms. The bond order analysis presented in the Table 2 confirm this graphical observation, where all of the Mg–Ti bond orders are smaller than 0.12. In all cases there is a hydrogen bridge between both metals. For these kinds of configurations, symmetry is almost non-existent. Fig. 6a shows that the hydrogenated structures have different geometries with optimized energy values very close to each other. Fig. 6b presents the hydrogenated isomers of the $TiMg_6$ cluster and the energy difference with respect to the minimum energy cluster. For example, the most stable cluster in singlete state is about 35 kcal/mol less stable than the corresponding triplet state. No structures were optimized in quintuplet state. This suggests that the triplet electronic state of the hydrogenated isomer is the most stable, even though the $TiMg_6$ cluster is in a different electronic state.

Fig. 6 shows that the hydrogen bond in these clusters can be classified in three types. There is a group of H atoms that act as a bridge between the Ti and Mg atoms. A second group of H atoms are bonded to two Mg atoms and a third group is formed by dangling H atoms bonded to one Mg atom. Each one of them has different bond lengths which indicates that in one cluster there are different bond energies which give rise to an energy distribution of the hydrogen–metal interaction. Therefore, hydrogen desorption should be in a range of temperatures where the hydrogen atoms more weakly bound will be the first to leave the cluster. The last hydrogen atoms would be very tightly bound and therefore would require large energies for desorption and longer reaction times. When the hydrogen atom is in between the Ti and Mg atoms (Ti–H–Mg), the distance between Ti–H is larger than the one between H–Mg suggesting a stronger interaction of the H atom with the Mg atom. This behavior can be related to the difference in electronegativity between the atoms involved in the bonding. However, these differences are reduced as the size of the cluster is increased, that is when increasing the number of Mg atoms in the cluster the Mg–H bond length increases, while the Ti–H distance is reduced or remain constant.

ELF analysis was carried out for the metallic hydrogenated clusters. An ELF value of 1 corresponds to perfect electron localization and an ELF value of 0.5 corresponds to the highest electron delocalization. Fig. 7 shows two isosurfaces for $TiMg_3$ and $TiMg_3H_8$ clusters. Fig. 7a corresponds to the 0.703 isosurface for $TiMg_3$ a set of basins located over each metallic atom and between them can be observed. The basins on the metallic atoms have an occupancy of 2.0 electrons, while those in between have an electronic density of 0.5 electrons. The location of these basins is close to the position of each hydrogen atom in the hydrogenated cluster. Fig. 7b shows the 0.900 isosurface for the $TiMg_3H_8$. This result is similar to the one reported by Cheng et al. [45] for bimetallic Ti–Pd systems, where the high ELF values between the Ti and Pd atoms correlate well with the location of the hydrogen atoms in the hydrogenated system. However, in our case the correlation is not as good because the Mg clusters show high relaxation as the hydrogen atoms are added to the structure.

The average bond order of the Ti–Mg bond is presented in Table 2. In the case of non-hydrogenated clusters the bond order has a trend to reduce its value with the size of the cluster indicating that the interaction Ti–Mg becomes weaker with the increase in the number of Mg atoms. When the clusters are hydrogenated there is

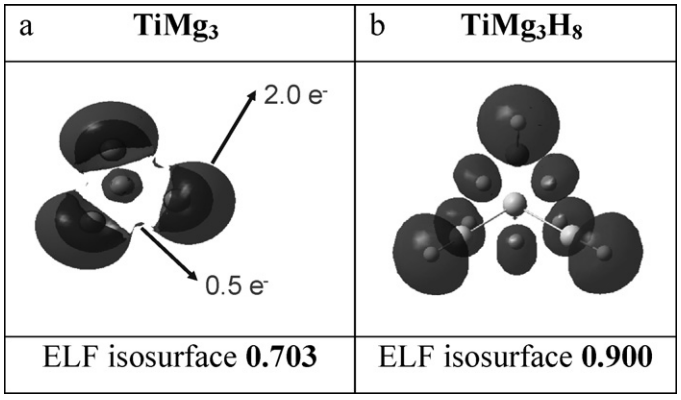

Fig. 7. ELF isosurface plots for $TiMg_3$ and $TiMg_3H_8$. In (a) the electronic density is located close to the metallic atoms or between them at an ELF value of 0.703. In (b) the electronic density is located over each hydrogen atom.

a clear reduction in the Ti–Mg bond order. As explained before, and shown in Fig. 6, in these clusters the hydrogen atom locates preferably between the Ti and Mg atoms forming a bridge between them. Therefore, the bond order is drastically reduced to values as low as 0.06 which is representative of very weak interactions between these atoms.

The location of the hydrogen atoms in the hydrogenated magnesium or titanium magnesium cluster, previously described, implies the migration of the hydrogen atoms to the innermost part of the cluster, and vice versa, in dehydrogenation the hydrogen atoms have to leave from those places to the outer part of the cluster to become molecular hydrogen. This process has a negative effect on the kinetics of the overall hydrogenation/dehydrogenation process using magnesium clusters.

3.3.4. *Dehydrogenation energy*

The dehydrogenation energies of the $TiMg_n$ and $Mg–Mg_n$ clusters shown in Fig. 8 indicate that dehydrogenation of bimetallic clusters is energetically more demanding that the magnesium clusters. The difference is more marked in the small size clusters, this gap becomes smaller as the size of the cluster increases. The large dehydrogenation energy of the small titanium clusters can be ascribed to the preference of the Ti atom to form more

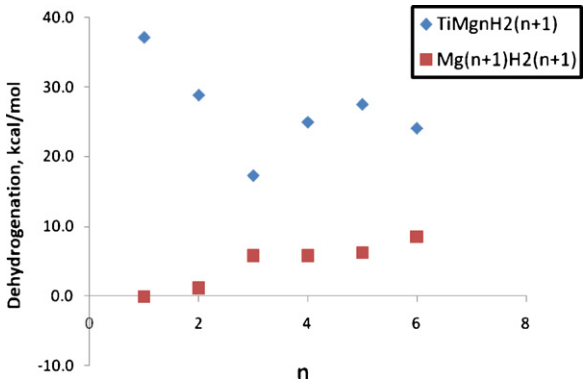

Fig. 8. Dehydrogenation energy of $TiMgnH_{2n}$ and $Mg–Mg_nH_{2n+2}$ clusters $XMg_nH_{2(n+1)} \rightarrow XMg_n + (n+1)H_2$.

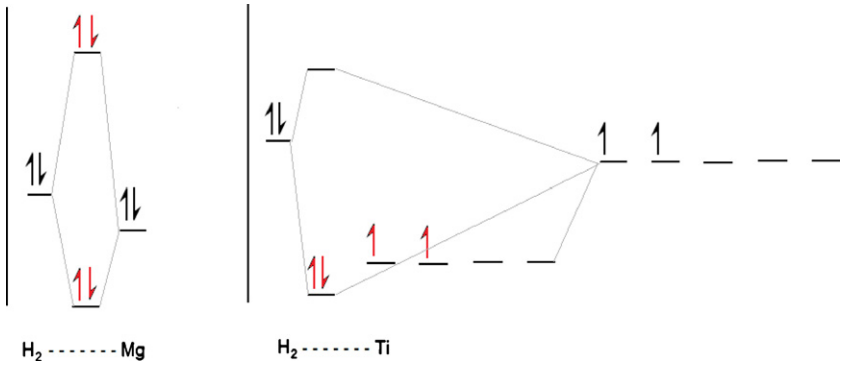

Fig. 9. Qualitative molecular orbital diagram of the interaction of molecular hydrogen and magnesium or titanium atoms.

stable interactions with the hydrogen atom than those formed with magnesium. For the Ti–Mg_nH_{2n+1} clusters, the dehydrogenation energy decreases as the number of Mg atoms increases while for the Mg_nH_{2n} clusters the dehydrogenation energy increases slightly.

In the case of small Mg clusters their interaction with molecular hydrogen is not favored because magnesium has a closed shell structure. While the interaction with the Ti–Mg_n clusters is positively favored. In this case the hydrogen molecule approaches the cluster by the Ti atom and since the Ti atom has vacancies in the valence orbitals there is a stronger interaction with these clusters. Fig. 9 shows a qualitative representation of a molecular orbital diagram for the interaction between a hydrogen molecule with a magnesium or titanium atom. As can be seen, the interaction H_2–Mg is a non-stabilizing one due to the presence of two electrons in bonding and antibonding orbitals. A different situation is observed for the interaction with Ti because this metal has unpaired electrons in the d orbital which facilitate the donation of the electrons of the σ orbital bonding of the molecular hydrogen to the metal atom; in this way the binding affinity between both species is enhanced, these kind of interactions strongly depend on the type of metal [46].

Another factor that can influence this interaction is the negative charge of the Ti metal which facilitates the overlapping of the electron density between both species and therefore a more stable complex is obtained.

On the contrary, the initial interaction of molecular hydrogen with the magnesium cluster is of the van der Waals type. As a consequence, stronger experimental conditions would be required to start the hydrogenation of a pure magnesium cluster compared to the conditions for the hydrogenation of a Ti–Mg_n cluster which should have more mild requirements of temperature.

4. Conclusion

The addition of titanium to magnesium clusters modifies the electronic characteristics of the Mg atoms. There is charge transfer from the Mg atoms to the Ti atom which causes a change in the electronic population of the s and p orbitals of the closest atoms to Ti in the bimetallic cluster. As a consequence, there is a complete change of the cluster reactivity sites. The above changes affect the kinetics and thermodynamics of the hydrogenation of the cluster. In particular there is a reduction in the energy barrier for the dissociation of the hydrogen molecule in the most stable bimetallic clusters.

On the other hand, it was observed that there are different types of hydrogen bonds inside a cluster as indicated by different bond lengths. Some of the isomers of the hydrogenated clusters have a very small energy difference between them which suggests that there may be a large variety of structures in a potential energy surface of hydrogenated bimetallic systems. The hydrogen atoms are preferentially located as bridges between the Mg atoms or between the Ti and Mg atoms in the cluster.

These simulated systems show tendencies that can be useful in the development of hydrogen storage systems. It is clear that with current technologies it is difficult to synthesize the isolated clusters. However, they can be produced in a dispersed way over a material with large surface area such as graphite, graphene, active carbon or carbon nanotubes.

Acknowledgements

The authors thank Colciencias and the University of Antioquia for financial support of the project No. 1115-405-20280. The authors also thank the University of Antioquia for funding of the "Sostenibilidad" Program (2009–2011). Gratitude is expressed to Dr. Elizabeth Florez for her advice on the Fukui calculations. W. Silva thanks Universidad de Antioquia-Municipio de Rionegro-Colciencias doctoral fellowship.

Appendix A. Supplementary data

Supplementary data associated with this article can be found, in the online version, at doi:10.1016/j.jallcom.2011.06.022.

References

[1] S. Shi, J.-Y. Hwang, International Journal of Hydrogen Energy 32 (2007) 224–228.
[2] M. Momirlan, T.N. Veziroglu, Renewable and Sustainable Energy Reviews 6 (2002) 141–179.
[3] G. Srinivas, Y. Zhu, R. Piner, N. Skipper, M. Ellerby, R. Ruoff, Carbon 48 (2010) 630–635.
[4] Y. Lin, F. Ding, B.I. Yakobson, Physical Review B 78 (2008) 041402.
[5] I. Cabria, M.J. López, J.A. Alonso, Physical Review B 78 (2008) 075415.
[6] P. Kondratyuk, J.T. Yates, Accounts of Chemical Research 40 (2007) 995–1004.
[7] B. Panella, K. Hönes, U. Müller, N. Trukhan, M. Schubert, H. Pütter, M. Hirscher, Angewandte Chemie International Edition 47 (2008) 2138–2142.
[8] G. Yang, L. Zhou, X. Liu, X. Han, X. Bao, The Journal of Physical Chemistry B 110 (2006) 22295–22297.
[9] M.J. van Setten, G.A. de Wijs, V.A. Popa, G. Brocks, Physical Review B 72 (2005) 073107.
[10] M. Au, Materials Science and Engineering B 117 (2005) 37–44.
[11] G. Wu, J. Zhang, Y. Wu, Q. Li, K. Chou, X. Bao, Applied Surface Science 256 (2009) 46–51.
[12] S.V. Alapati, J.K. Johnson, D.S. Sholl, Physical Review B 76 (2007) 104108.
[13] J. Lu, Z.Z. Fang, H.Y. Sohn, The Journal of Physical Chemistry B 110 (2006) 14236–14239.
[14] D. Kyoi, N. Kitamura, H. Tanaka, A. Ueda, S. Tanase, T. Sakai, Journal of Alloys and Compounds 428 (2007) 268–273.
[15] D.K. Ross, Vacuum 80 (2006) 1084–1089.
[16] M.A. Lillo-Ródenas, Z.X. Guo, K.F. Aguey-Zinsou, D. Cazorla-Amorós, A. Linares-Solano, Carbon 46 (2008) 126–137.
[17] S.B. Kalidindi, B.R. Jagirdar, Inorganic Chemistry 48 (2009) 4524–4529.
[18] M. Polanski, J. Bystrzycki, Journal of Alloys and Compounds 486 (2009) 697–701.
[19] S. Cheung, W.-Q. Deng, A.C.T. van Duin, W.A. Goddard, The Journal of Physical Chemistry A 109 (2005) 851–859.

[20] R.W.P. Wagemans, J.H. van Lenthe, P.E. de Jongh, A.J. van Dillen, K.P. de Jong, Journal of the American Chemical Society 127 (2005) 16675–16680.
[21] J.J. Reilly, R.H. Wiswall, Inorganic Chemistry 6 (1967) 2220–2223.
[22] J.J. Reilly, R.H. Wiswall, Inorganic Chemistry 7 (1968) 2254–2256.
[23] L. Baum, M. Meyer, L. Mendoza-Zélis, Physica B: Condensed Matter 389 (2007) 189–192.
[24] D.W. Zhou, S.L. Li, R.A. Varin, P. Peng, J.S. Liu, F. Yang, Materials Science and Engineering: A 427 (2006) 306–315.
[25] G. Liang, J. Huot, S. Boily, A. Van Neste, R. Schulz, Journal of Alloys and Compounds 291 (1999) 295–299.
[26] N. Hanada, T. Ichikawa, H. Fujii, The Journal of Physical Chemistry B 109 (2005) 7188–7194.
[27] J. Chen, H.-B. Yang, Y.-Y. Xia, N. Kuriyama, Q. Xu, T. Sakai, Chemistry of Materials 14 (2002) 2834–2836.
[28] K. Asano, H. Enoki, E. Akiba, Journal of Alloys and Compounds 486 (2009) 115–123.
[29] A.J. Du, S.C. Smith, X.D. Yao, G.Q. Lu, The Journal of Physical Chemistry B 109 (2005) 18037–18041.
[30] Y. Song, Z.X. Guo, R. Yang, Physical Review B 69 (2004) 094205.
[31] Y. Luo, P. Wang, L.-P. Ma, H.-M. Cheng, Scripta Materialia 56 (2007) 765–768.
[32] D. Chen, Y.M. Wang, L. Chen, S. Liu, C.X. Ma, L.B. Wang, Acta Materialia 52 (2004) 521–528.
[33] J. Akola, K. Rytkönen, M. Manninen, European Physical Journal D 16 (2001) 21–24.
[34] V. Kumar, R. Car, Physical Review B 44 (1991) 8243.
[35] W.Q. Tian, M. Ge, F. Gu, Y. Aoki, The Journal of Physical Chemistry A 109 (2005) 9860–9866.
[36] G.W.T.M.J. Frisch, H.B. Schlegel, G.E. Scuseria, J.R.C.M.A. Robb, J.A. Montgomery Jr., T. Vreven, J.C.B.K.N. Kudin, J.M. Millam, S.S. Iyengar, J. Tomasi, B.M.V. Barone, M. Cossi, G. Scalmani, N. Rega, H.N.G.A. Petersson, M. Hada, M. Ehara, K. Toyota, J.H.R. Fukuda, M. Ishida, T. Nakajima, Y. Honda, O. Kitao, M.K.H. Nakai, X. Li, J.E. Knox, H.P. Hratchian, J.B. Cross, C.A.V. Bakken, J. Jaramillo, R. Gomperts, R.E. Stratmann, A.J.A.O. Yazyev, R. Cammi, C. Pomelli, J.W. Ochterski, K.M.P.Y. Ayala, G.A. Voth, P. Salvador, J.J. Dannenberg, S.D.V.G. Zakrzewski, A.D. Daniels, M.C. Strain, D.K.M.O. Farkas, A.D. Rabuck, K. Raghavachari, J.V.O.J.B. Foresman, Q. Cui, A.G. Baboul, S. Clifford, B.B.S.J. Cioslowski, G. Liu, A. Liashenko, P. Piskorz, R.L.M.I. Komaromi, D.J. Fox, T. Keith, M.A. Al-Laham, A.N.C.Y. Peng, M. Challacombe, P.M.W. Gill, W.C.B. Johnson, M.W. Wong, C. Gonzalez, J.A. Pople, Gaussian 03, Revision E. 01, 2004.
[37] A. Lyalin, I.A. Solov'yov, A.V. Solov'yov, W. Greiner, Physical Review A 67 (2003) 063203.
[38] J. Christopher, D.G. Cramer, Truhlar, Physical Chemistry Chemical Physics 11 (2009) 10757–10816.
[39] Z.J. Wu, Y. Kawazoe, Chemical Physics Letters 423 (2006) 81–86.
[40] a. Robert, G. Parr, W. Yang, Density-Functional Theory of Atoms and Molecules, Oxford Science Publications, New York, 1989.
[41] R.G. Parr, International Journal of Quantum Chemistry 26 (1984) 687–692.
[42] S.K. Noury, X. Fuster, F.B. Silvi, Top-Mod, University P. M. Curie, Paris, 1997.
[43] A. Kaufmann, A. Kornath, A. Zoermer, R. Ludwig, Inorganic Chemistry 49 (2010) 3851–3856.
[44] W.J. Balfour, Journal of Physics B: Atomic and Molecular Physics 3 (1970) 1749.
[45] X.-Q. Chen, C.L. Fu, J.R. Morris, Intermetallics 18 (2010) 998–1006.
[46] R.C. Lochan, M. Head-Gordon, Physical Chemistry Chemical Physics 8 (2006) 1357–1370.